NASA/TM—2018-220003

An Overview of High Bandwidth Liquid Fuel Flow Modulators Developed for Active Combustion Control Research

Joseph R. Saus and Randy Thomas
Glenn Research Center, Cleveland, Ohio

December 2018

NASA STI Program . . . in Profile

Since its founding, NASA has been dedicated to the advancement of aeronautics and space science. The NASA Scientific and Technical Information (STI) Program plays a key part in helping NASA maintain this important role.

The NASA STI Program operates under the auspices of the Agency Chief Information Officer. It collects, organizes, provides for archiving, and disseminates NASA's STI. The NASA STI Program provides access to the NASA Technical Report Server—Registered (NTRS Reg) and NASA Technical Report Server—Public (NTRS) thus providing one of the largest collections of aeronautical and space science STI in the world. Results are published in both non-NASA channels and by NASA in the NASA STI Report Series, which includes the following report types:

- TECHNICAL PUBLICATION. Reports of completed research or a major significant phase of research that present the results of NASA programs and include extensive data or theoretical analysis. Includes compilations of significant scientific and technical data and information deemed to be of continuing reference value. NASA counter-part of peer-reviewed formal professional papers, but has less stringent limitations on manuscript length and extent of graphic presentations.

- TECHNICAL MEMORANDUM. Scientific and technical findings that are preliminary or of specialized interest, e.g., "quick-release" reports, working papers, and bibliographies that contain minimal annotation. Does not contain extensive analysis.

- CONTRACTOR REPORT. Scientific and technical findings by NASA-sponsored contractors and grantees.

- CONFERENCE PUBLICATION. Collected papers from scientific and technical conferences, symposia, seminars, or other meetings sponsored or co-sponsored by NASA.

- SPECIAL PUBLICATION. Scientific, technical, or historical information from NASA programs, projects, and missions, often concerned with subjects having substantial public interest.

- TECHNICAL TRANSLATION. English-language translations of foreign scientific and technical material pertinent to NASA's mission.

For more information about the NASA STI program, see the following:

- Access the NASA STI program home page at http://www.sti.nasa.gov

- E-mail your question to help@sti.nasa.gov

- Fax your question to the NASA STI Information Desk at 757-864-6500

- Telephone the NASA STI Information Desk at 757-864-9658

- Write to:
  NASA STI Program
  Mail Stop 148
  NASA Langley Research Center
  Hampton, VA 23681-2199

NASA/TM—2018-220003

An Overview of High Bandwidth Liquid Fuel Flow Modulators Developed for Active Combustion Control Research

Joseph R. Saus and Randy Thomas
Glenn Research Center, Cleveland, Ohio

National Aeronautics and
Space Administration

Glenn Research Center
Cleveland, Ohio 44135

December 2018

Acknowledgments

The authors wish to acknowledge the following NASA Glenn Research personnel who have participated in the development of the work presented in this paper: John C. DeLaat, Clarence T. Chang, Kathleen M. Tacina, Daniel E. Paxson, Daniel R. Vrnak, Thomas J. Stueber, George Kopasakis, and Jeffrey Hamman.

Level of Review: This material has been technically reviewed by technical management.

Available from

NASA STI Program
Mail Stop 148
NASA Langley Research Center
Hampton, VA 23681-2199

National Technical Information Service
5285 Port Royal Road
Springfield, VA 22161
703-605-6000

This report is available in electronic form at http://www.sti.nasa.gov/ and http://ntrs.nasa.gov/

An Overview of High Bandwidth Liquid Fuel Flow Modulators Developed for Active Combustion Control Research

Joseph R. Saus and Randy Thomas
National Aeronautics and Space Administration
Glenn Research Center
Cleveland, Ohio 44135

Abstract

This paper presents a description of the general construction of three high bandwidth liquid fuel modulators along with data corresponding to their respective modulation performance. These devices are a critical element of the National Aeronautics and Space Administration Glenn Research Center's (NASA GRC) Active Combustion Control (ACC) task. These devices are not commercially-off-the-shelf available, primarily due to a 1 kHz bandwidth requirement. Given their special nature, NASA GRC developed specifications for the modulation devices and then, through Small Business Innovative Research (SBIR) contracts, had vendors with expertise in valve design manufacture them. The modulators described in this paper are the Active Signal Modulator (ASM), the Jansen's Aircraft System Controls (JASC) modulator, and the WASK Engineering (WASK) modulator. These modulators utilize magnetostrictive, electric motor, or piezoelectric actuation, respectively. The specifications for these devices evolved over time to meet the needs of changing objectives in the ACC research task. This is primarily true with respect to flow number as their designs accommodate a range from 1 to 8 ($lbm/hr\text{-}psi^{0.5}$). These designs also exhibit relatively small volume, weight, and power consumption with an ability to modulate approximately ±30 percent from the mean on a pressure basis. The modulators have been characterized and have undergone laboratory performance tests by the vendors. Their data indicated suitability for continued use in ACC research testing.

Introduction

In response to increasingly strict limitations on emission output levels for both land-based and aircraft gas turbine engines, combustion research has focused on premixed lean combustion designs. However, these lean-burning concepts have shown an increased susceptibility to combustion instabilities (Refs. 1 to 5). These instabilities can cause combustor pressure oscillations which lead to premature mechanical failure. They are characterized by a coupling (i.e., mutual reinforcement) of the combustion heat release perturbations with the inherent combustor geometry acoustic pressure perturbations (thermo-acoustic instabilities). Ideally, passive techniques would be the most attractive solution to solve these problems because they minimize weight and component count, but given the extent of dynamic conditions that occur over the complete mission cycle of an aircraft engine, passive techniques may not be fully successful. Additionally, passive techniques can add to combustor losses, and must be "designed in" whereas active approaches can be used on existing designs. For this reason, it becomes prudent to also investigate Active Combustion Control (ACC) techniques (Refs. 6 to 19).

The ACC concept addresses the instability mechanism previously mentioned. The basic approach is to modulate and control the fuel flow (Refs. 15 to 18) through the combustor fuel injector(s) to disrupt the coupling and suppress the pressure oscillations. In previous ACC research (Ref. 19), combustion instability was successfully suppressed by modulation of the fuel through the main fuel injectors. The question remains, however, of whether or not successful instability suppression can be accomplished by modulating a smaller percentage of the total fuel supply through the pilot(s) injectors. If so, it would offer certain advantages in terms of emissions reduction. It would also permit the development of potentially smaller, lighter, and less power demanding modulation devices that can be integrated into the injector

assemblies. For the purpose of answering this question, the fuel modulators described here have been designed and developed to modulate fuel flows that are appropriate for pilot injectors.

For the instability suppression demonstrated in the past at the National Aeronautics and Space Administration Glenn Research Center (NASA GRC), fuel modulation was applied to the greater percentage of fuel flowing through the main injectors. In this application a magnetostrictive actuation device developed by the Georgia Institute of Technology was utilized. This device was designed to accommodate a nominal flow number (FN) of 110 (lbm/hr-psi$^{0.5}$). Later, the research focus changed and was redirected at demonstrating combustor pressure modulation and potential for active instability suppression through modulation of the pilot flow, which had a flow number of 8 (lbm/hr-psi$^{0.5}$). The results for this application, using the same Georgia Tech modulator, were not as good (Ref. 19). For this reason additional modulators were sought which were designed more appropriately for the lower flow number range of 1 to 8 (lbm/hr-psi$^{0.5}$). Equation (1) provides the definition of FN. It is simply the ratio of mass flow rate, $\dot{m}$, in lbm/hr to the square root of the pressure difference, ΔP, in psi across an orifice (akin to flow coefficient, Cv, in fluid mechanics). The remainder of this report will state flow numbers without units, but it should be understood that the units of (lbm/hr-psi$^{0.5}$) apply.

$$\mathrm{FN} = \frac{\dot{m}}{\sqrt{\Delta P}} \tag{1}$$

Successful control of combustion instabilities through pilot fuel modulation will depend on whether the percentage of fuel modulation is sufficient to effect the combustor instability pressure and whether the modulator, through its connecting fuel line system, exhibits sufficient modulation strength at that frequency to attempt closed loop control. In the body of research to date, combustion instabilities in gas turbine engines have generally been observed in the 300 to 1000 Hz range (military engines have encountered some even higher frequencies). Unfortunately, actuators with this bandwidth are not available as off-the-shelf manufactured items so it becomes necessary to develop custom fuel actuators. NASA GRC opted to develop specifications for 'low' FN, high bandwidth modulators and then used outside vendors to develop such devices.

The remainder of this paper will focus on the three high bandwidth fuel modulators developed for NASA GRC's ACC research concerned with modulating combustor pilot fuel flow. These modulators are: Active Signal Technologies Modulator, Jansen's Aircraft System Controls Modulator, and WASK Engineering Modulator. For each, specifications will be presented along with a brief description of its physical construction and then data that provides a measure of its performance. Unfortunately, a direct comparison between the measures of performance for each modulator cannot be made because the data presented are not obtained from a common flow bench. In lieu of this shortcoming, the paper will close with general conclusions about the performance and reliability of each modulator with respect to its conceptual makeup, and a projection of their use in future work.

The Active Signal Technologies Modulator (ASM)

New modulator design specifications were drafted by NASA GRC and incorporated into a 2008 Small Business Innovative Research (SBIR) solicitation. These specifications are shown in Table 1.

TABLE 1.—ACTIVE SIGNAL MODULATOR DESIGN SPECIFICATIONS

Maximum mean flow rate	90 lbm/hr
Flow number range	3 to 8
Inlet pressure range	400 to 1000 psi
Minimum outlet pressure	250 psi
Desired modulation	±40% of mean mass flow
Minimum bandwidth	1000 Hz
Flow media	Water, JP-8 jet fuel
Maximum operating temperature	300 °F
Failure mode	Open

In response to the SBIR solicitation a proposal submitted by Active System Technologies (AST) was awarded. They partnered with Moog, Inc. to develop and construct a magnetostrictive-based modulator (to be referred to as the ASM). They were awarded a Phase I contract and later a contract through a Combustion NASA Research Announcement (NRA). Figure 1 shows an annotated view of the modulator exterior that identifies its main elements. The provided scale indicates its dimensions to be about 17.5 by 3 by 3 in.; its weight is about 11 lb. The size and weight of the ASM is comparable to that of the Georgia Tech Valve (GTV). Figure 2 shows an annotated cutaway drawing of the ASM. From the drawing one can observe the basic construction of the modulator and identify three distinct functional sections: Dry End, Wet End, and Stepper Motor/Optical Encoder.

It is beyond the scope of this document to provide a comprehensive engineering description for any of the modulation devices being discussed herein. That information can be found in the vendor's Final reports and for the ASM they are cited in References 20 and 21. These reports are not publicly available. To secure a copy of these references, the reader must contact the contractor directly and make a formal request through them. The reference they provide may be redacted in some respects in order to protect information they consider proprietary. The contractor's address is provided as part of the reference as a convenience. The following brief general description of its operation is provided to permit better understanding without disclosing any proprietary information.

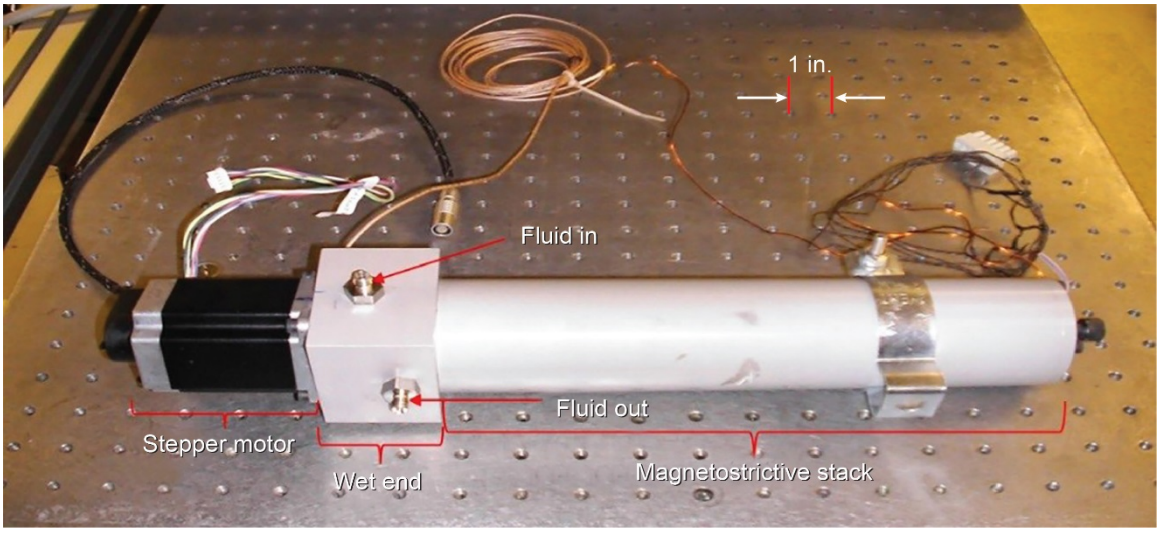

Figure 1.—The Active Signal Modulator (ASM).

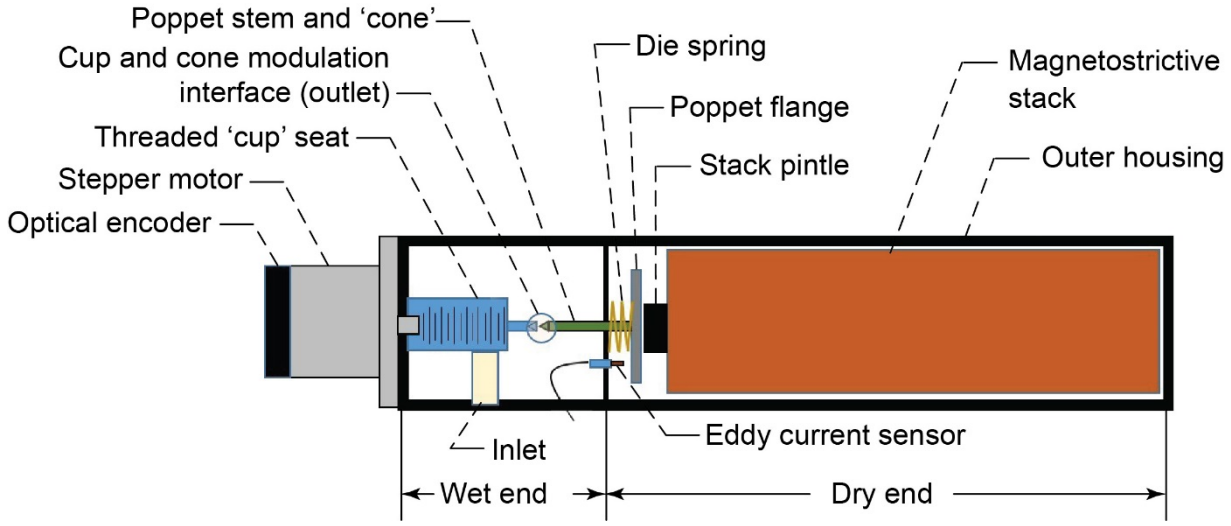

Figure 2.—Schematic Cutaway View of the ASM.

The ASM is driven by a current-source sinusoidal signal that is generated as the result of amplifying and converting the voltage output of a signal generator (ranging from 1 to 3 V p-p). A custom-built control box, provided by AST, serves as an interface between the amplifier output and the magnetostrictive stack. In response to the 'command' signal delivered by the signal generator, the stack components (comprised in large part of Terfenol D) undergo a cyclic crystallographic plane straining and restoring in accordance with the user specified sinusoidal amplitude and frequency. The amplitude of the sinusoid is directly related to the magnitude of the induced strain that is ultimately observed as the axial displacement of the stack. To prevent the Terfenol D from experiencing inelastic straining, a limit must be imposed on the user-specified amplitude for the sinusoid to avoid any permanent deformation. Bench tests conducted at AST indicated a maximum achievable displacement of 4.8 mils p-p for a thermally-limited amplitude specification that does not exceed 14 A p-p. For issued command signals adhering to this limitation, the resulting stack displacement imparts a force, via an attached pintle, onto the poppet flange. Integral to the poppet flange is the poppet ('cone') whose corresponding displacement acts to change the effective flow area between itself and the seat ('cup'). A die spring is used as a restoring force for the stack; the stack is installed with a preload on the spring to optimize operation. The mean flow condition for a test operation is created by the movement of the seat, via the stepper motor, to set the spatial distance between itself and the poppet when there isn't any modulation occurring. Operation of the modulator after the mean condition is established will induce thermal growth within the stack due to heating resulting from the high frequency cyclic motions. For this reason a mean flow controller is used to command the stepper motor to adjust the spatial distance between itself and the poppet in order to compensate for the growth, thereby maintaining the proper mean flow condition. An eddy current sensor that measures the displacement of the poppet flange is used as feedback for this controller.

Performance tests were conducted at NASA GRC using a flow bench that used city water as the working fluid. The essence of the flow bench test section is depicted in Figure 3. In that figure a coriolis principle-based flow meter, a bladder accumulator, the test candidate, a variable length tube, a needle valve, and pressure transducer instrumentation are identified as the main constituent components. In general, the rationale for the circuit design is to provide a quiescent fluid source to the test candidate as it operates on that fluid, and then introduce an orifice downstream, acting as a simulated fuel injector, to receive the candidate's modulated output. In so doing, the circuit approximates the modulator's installation on a combustion research rig sans the flame. An elaboration of this circuit functionality follows.

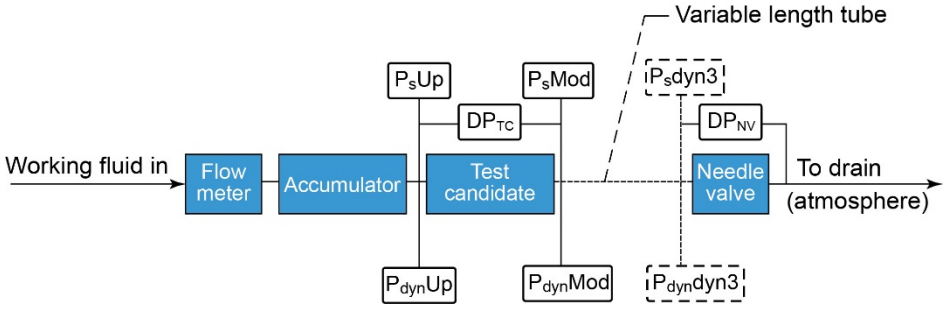

Figure 3.—NASA Flow Bench Test Section.

The working fluid is supplied to the test section by a positive displacement piston pump. This type of pump type introduces ‘pressure noise’ over a broad range of frequencies due to the reciprocating motion of the pistons. To eliminate this unwanted noise, the pumped fluid is passed through the bladder accumulator to dampen (filter) the pressure oscillations before it is introduced to the test candidate. The test candidate, being issued a sinusoidal command, operates on the fluid to produce a sinusoidal output having the same frequency as the command (the output’s amplitude will vary as a function of frequency). The sinusoidal output continues to travel downstream to a needle valve, which has a variable orifice and serves as a simulated fuel injector. The fluid then passes from the needle valve to a drain at atmospheric pressure. The test section has two configurations. The first configuration has a very short or ‘minimum’ length separation between the modulator exit port and the orifice. This is referred to as the ‘short configuration’ where the test candidate output port is closely connected to the needle valve (the transducers labeled $P_s$dyn3 and $P_d$dyn3 are not used). The data collected in this configuration is considered baseline data since the performance of the modulator is the best it can be as it is not degraded by line losses due to capacitance and/or inductance brought on by the extra length of travel. Note the internal diameters (ID’s) of compression fittings, etc., are not necessarily the same as that of the fluid line, in which case the performance of the setup can be further improved. The second configuration, referred to as the ‘long configuration’, involves using various lengths of tube between the modulator output and the needle valve. Line lengths of 24 and 53 in. were typically used. The data collected in this arrangement permitted measurement of the modulator’s output degradation due to traveling the extra length of tube to the needle valve.

Discrete perturbation tests were conducted that subjected the modulator to sinusoidal commands having a fixed signal generator amplitude of 1.5 V peak. An independent measurement taken during testing showed this setting resulted in a current input that didn’t exceed the 7 A peak current limit that the modulator can safely accept. The commands were issued with frequencies in the discrete range of 100 to 1000 Hz in 100 Hz increments. Separate transducers were used to measure the dc and ac components of the absolute pressure. The transducers labeled an ‘s’ subscript pertain to dc measurements whereas the transducers labeled with a ‘dyn’ subscript pertain to the ac measurement. Separate differential pressure transducers were used to measure the pressure difference across the modulator and the needle valve. These measurements were used together with the mass flow rate measurements and Equation (1) to calculate the respective flow numbers (FN_{TC} and FN_{NV} – TC referring to Test Candidate, NV referring to Needle Valve). Table 2 presents a summary of the dc conditions common to all the tests.

Representative baseline (tube length = min) data is presented in Figure 4 for the 100, 500, and 1000 Hz tests. The plots present power spectra for corresponding pressure time traces of the P_{dyn}Mod measurement. The power spectrum is generated in MATLAB (The Mathworks, Inc., Natick, MA) using the Pwelch command to get the Power Spectral Density (PSD). In general, the data confirms that the dominant frequency in each case is that of the commanded frequency. Harmonics (and subharmonics) are also present, but their magnitude is 20 percent or less of that at the dominant frequency. Because the harmonics present are even and odd frequencies of the fundamental, it is believed that these harmonics are due to the piping downstream of the modulator rather than from noise introduced by the pump. Perhaps they are due to reflections from variations in the flow areas in the piping. Also, PSD plots of PdynUp were examined with the modulator at rest and the data showed magnitudes of less than 0.2 across the frequency range.

TABLE 2.—SUMMARY OF TEST CONDITIONS FOR PERTURBATION TESTS

Tube length, in.	Mass flow rate, lbm/hr	P_sUp, psi	P_sMod, psi	DP_{TC}, psid	P_sDyn3, psi	DP_{NV}, psid	FN_{TC}, $lbm \cdot hr^{-1} \cdot psi^{-0.5}$	FN_{NV}, $lbm \cdot hr^{-1} \cdot psi^{-0.5}$
min	33.2	160.0	82.3	77.4	----	68.0	3.8	4.0
24	32.6	160.0	83.0	77.2	82.3	67.4	3.7	4.0
53	32.5	160.0	82.7	77.4	81.9	67.1	3.7	4.0

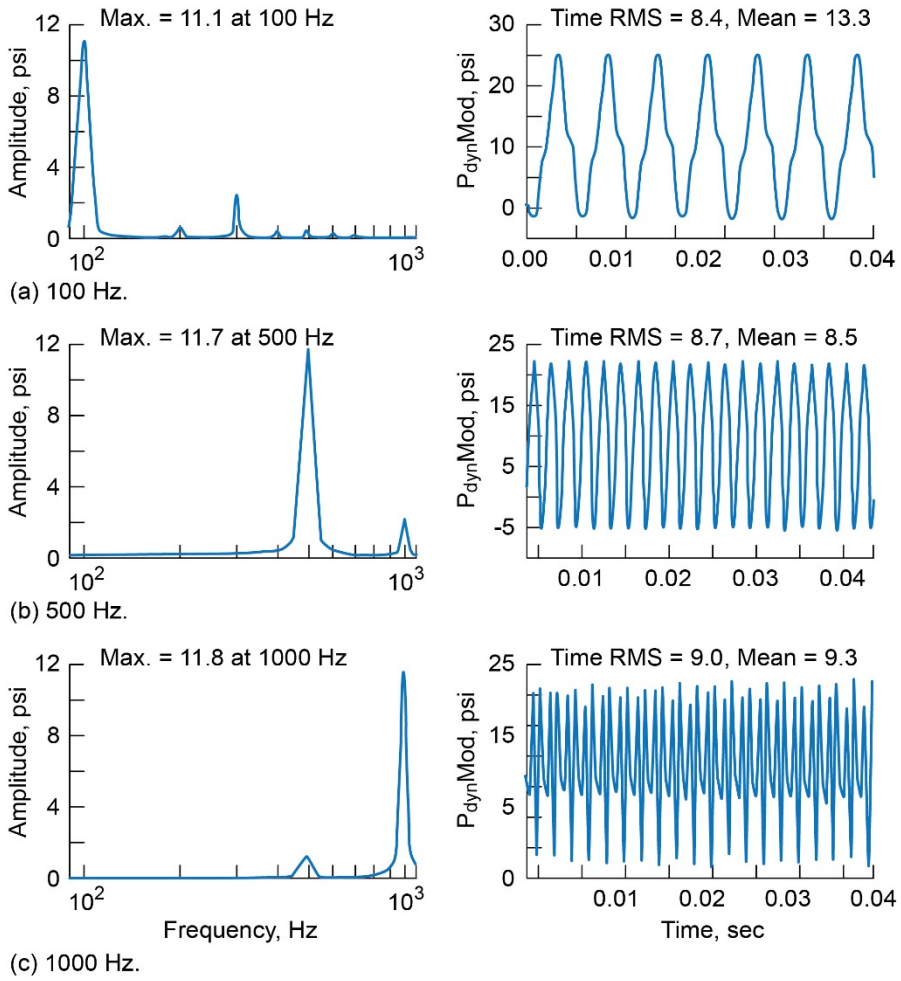

Figure 4.—ASM Performance Data for P_{dyn}Mod at 100, 500, and 1000 Hz.

For making an assessment of modulator performance, the PSD amplitude of the modulator output fuel pressure at the commanded frequency is an important criterion. The higher the amplitude of this pressure signal, the higher the likelihood that a healthy fuel pressure signal will be delivered to the injector inlet and therefore, the higher the likelihood that the combustor instability can be controlled (Ref. 16). It is also important that this PSD pressure signal is free of noise like harmonics, etc., so that the modulator can closely follow the sinusoidal input command within the desired frequency bandwidth of the modulator, without exciting unwanted combustor frequencies. Figure 4 shows PSD responses of the modulator at discrete frequencies with amplitudes which are qualitatively considered to be relatively acceptable (not too weak but not too strong either), however, with a significant amount of distortion present as it can be seen in both the frequency and time domain responses. So overall, the performance of this modulator is somewhat concerning, except perhaps for its performance at 500 Hz.

The performance of the modulator can also be assessed relative to its ability to modulate the mass flowrate within the desired frequency bandwidth, since, ultimately, it's the fuel mass flowrate modulation in the combustor that is generating the pressure wave that is used to control the instability. Thus, the amplitude of this mass flowrate modulation can be an additional performance measure. For the total mass flowrate modulation strength which is considered here, however, its harmonic content is not accounted for and for that the pressure PSD provides for this information.

For the 100 Hz case, the modulation strength from a pressure sense (time domain) is about 8.4 psi rms and the ac mean is approximately 13.3 psi. In order to determine the modulation strength on a mass basis, the ac measurement must be corrected by the actual mean pressure as reported by P_sMod in Table 2. For the 100 Hz case the actual mean is 82.3 psi and the corresponding maximum and minimum pressures become 95.6 psi (82.3 psi + 13.3 psi) and 69 psi (82.3 psi – 13.3 psi), respectively. The pressure on the downstream side of the needle valve is 14.7 psi (atmospheric pressure). The mass modulation strength is determined from Equation (2) as a percent difference between the maximum (or minimum) mass flow rate and the mean mass flow rate.

$$\%\,\text{Mass Modulation Strength} = \left| \frac{\dot{m}_{\max}\,(\text{or}\,\min) - \dot{m}_{\text{mean}}}{\dot{m}_{\text{mean}}} \right| \times 100\% \tag{2}$$

These mass flow rates are obtained by using Equation (1) together with the flow number across the needle valve and (separately) the pressure differences generated by subtracting atmospheric pressure from the maximum, mean, and minimum pressures. Table 3 summarizes the mass modulation strength for the plots shown in Figure 4. The data indicates that the modulation strength is about 8 percent on the positive stroke with a possible increase due to a resonance occurring around 500 Hz. For the negative stroke the data appears to indicate that modulation strength decreases with an increase in frequency. No explanation is immediately available to account for this asymmetric behavior.

The measured modulation strength has significance when considering the ultimate goal of ACC which is to influence the combustor pressure near the instability frequency to allow for active suppression of combustor dynamics. Ultimately, the goal may be to integrate these types of modulators into the injector assemblies, but to date, all tested modulators have been installed at a remote location relative to the fuel injector of a research combustor. Therefore, for this part of the research the transmission of a modulator fuel pulse must be strong enough to overcome the attenuations incurred by the different flow areas or by the line length leading to the fuel injector (could be on the order of approximately 20 to 36 in.). It is for this reason that tests are conducted which introduce additional separation distance between the modulator and the simulated fuel injector. Pressure measurements are made at the modulator exit and at the inlet to the injector (needle valve) so that a comparison can be made to determine any degradation in performance.

Figure 5 presents data that compares baseline and extended line length performance. The plot represents the average result from several tests where tube lengths of approximately 0, 24, and 53 in. were used. For all the perturbation tests conducted, the maximum pressure amplitude determined by the PSD at a given test frequency was recorded at the needle valve inlet. These recorded values at each frequency were averaged to obtain a representative value. The result of this process showed virtually no distinct difference in the performance for the extended tube lengths of 24 and 53 in. Therefore, a single ‘curve’ is presented that represents the performance of the extended tube lengths. The representative points have been connected by smooth lines. Also presented in the figure is a companion plot that shows the variance in the data points at a given frequency.

Some general observations that can be made from the plots in Figure 5 are as follows. First, the maximum pressure amplitude for the baseline data tends to decrease with frequency for the lower end of the frequency range. In moving from 400 Hz, however, the amplitude increases due to the valve mechanical resonance. In moving from 600 to 1000 Hz the trend is, in general, a decrease in amplitude.

TABLE 3.—SUMMARY OF MASS MODULATION STRENGTH

Freq., Hz	P_{RMS}, psi	P_{mean}, psi	P_sMod, psi	P_{max}, psi	P_{min},, psi	FN_{NV},, lbm/hr·psi$^{0.5}$	$\dot{m}_{max}$, lbm/hr	$\dot{m}_{mean}$, lbm/hr	$\dot{m}_{min}$, lbm/hr	$\%\dot{m}_{max}$	$\%\dot{m}_{min}$
100	8.4	13.3	82.3	95.6	69.0	4	36.0	33.2	29.5	8.4	11.1
500	8.7	13.5	83.0	96.5	69.5	4	36.2	32.6	29.6	11.0	9.2
1000	9.0	9.3	82.7	92.0	73.4	4	35.2	32.5	30.6	8.3	5.8

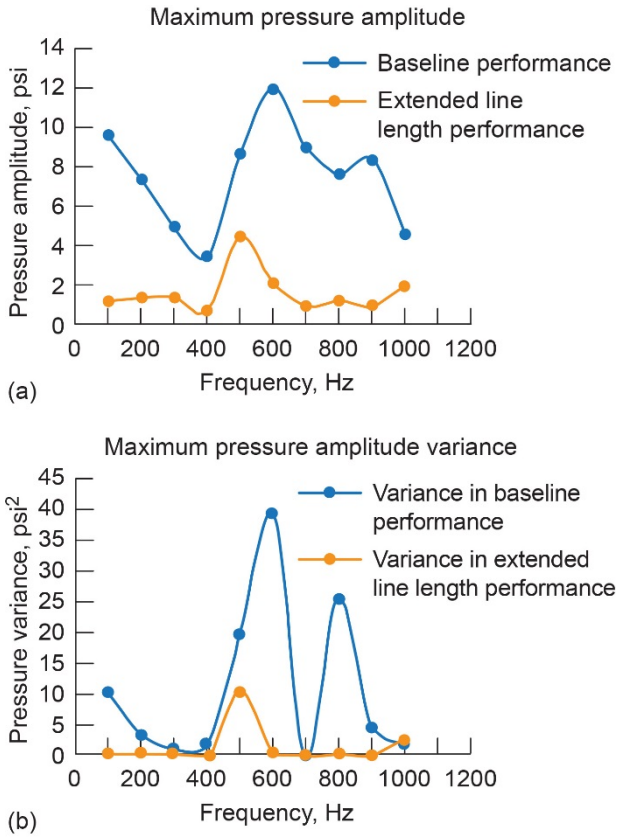

Figure 5.—ASM Performance Comparison for pressure measurements recorded at the needle valve inlet. (a) Maximum pressure amplitude. (b) Maximum pressure amplitude variance.

The data for the extended line lengths has a fairly flat performance trend at an amplitude below 2 psi. It does, however, parallel the baseline data with an increase in amplitude from approximately 400 to 600 Hz. However, the amplitude decrease after the resonance begins sooner than the baseline data and resumes its flat performance at below 2 psi. Actual tests with a combustion research rig would be required to determine if the lower amplitude performance would be sufficient to influence the combustion process favorable for active combustion control, especially when modulating pilot flow. The variance for the extended length performance data is shown to be quite small except at 500 Hz where the resonant condition occurs. The variance for the baseline data exhibits more swings, most notably at the frequency ranges of approximately 550 to 650 Hz, and 750 to 850 Hz.

The Jansen Aircraft System Controls Modulator (JASC)

In 2009, the ACC research task had begun considering the use of Lean Direct Injection (LDI) arrays for fuel modulation. The number of injectors in a given array could vary, but typically they numbered 6 to 9. Each injector had a flow number of around 1.0, but the composite flow number is additive if multiple injectors were fed modulated fuel. To accommodate the ACC research applications involving LDI's, additional modulators were needed in order to accommodate the lower flow number LDI application (using a single or composite injectors). In 2009 specifications were again included in another SBIR solicitation that were identical to those already shown in Table 1 with the exception of the flow number range which was narrowed to be between 3 and 5. A proposal was accepted from Jansen's Aircraft System Controls (JASC) for a modulator design and it received both Phase I and Phase II awards. Figure 6 shows the modulator delivered by JASC resulting from that effort along with a schematic

depiction that provides an indication of its size (about 4.1 by 2.5 by 2 in.). Its weight is about 2 lb. In comparison to the two magnetostrictive predecessors, this modulator design represents an 87 percent reduction in size and about an 84 percent reduction in weight.

Figure 7 shows a cutaway view of this modulator which was patented under US 8,650,880 B1. It is intended to serve as a reference for the general description of its operation that follows.

This design accomplishes modulation by slinging fluid from a set of flutes, attached to one end of a rotating shaft, through stationary flow windows. Modulation frequency is controlled by the rotational speed of the flutes; mass flow rate and modulation amplitude are controlled by the translation of the flutes across stator windows which impacts the percentage of the open flow area. Rotation of the shaft is accomplished by an electric motor and translation of the shaft is accomplished by the use of a proportional solenoid. A novel transducer, referred to as the Linear Variable Transducer Resolver, (LVTRx), was developed for this device that measures both rotation and translation of the shaft and constitutes a source of feedback for the controller used to command its operation. This modulator was intended to operate with a supply of fuel, a source of electrical power, and signal generator. A custom

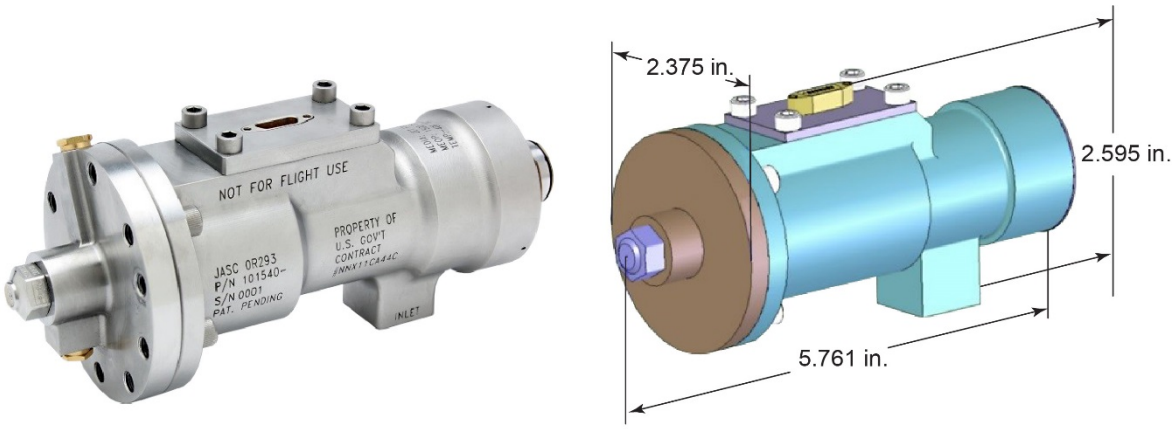

(a) The JASC modulator. (b) Dimensional view of the JASC modulator.

Figure 6.—Views of the JASC Modulator (from Ref. 23). (a) The JASC Modulator. (b) Dimensional view of the JASC Modulator.

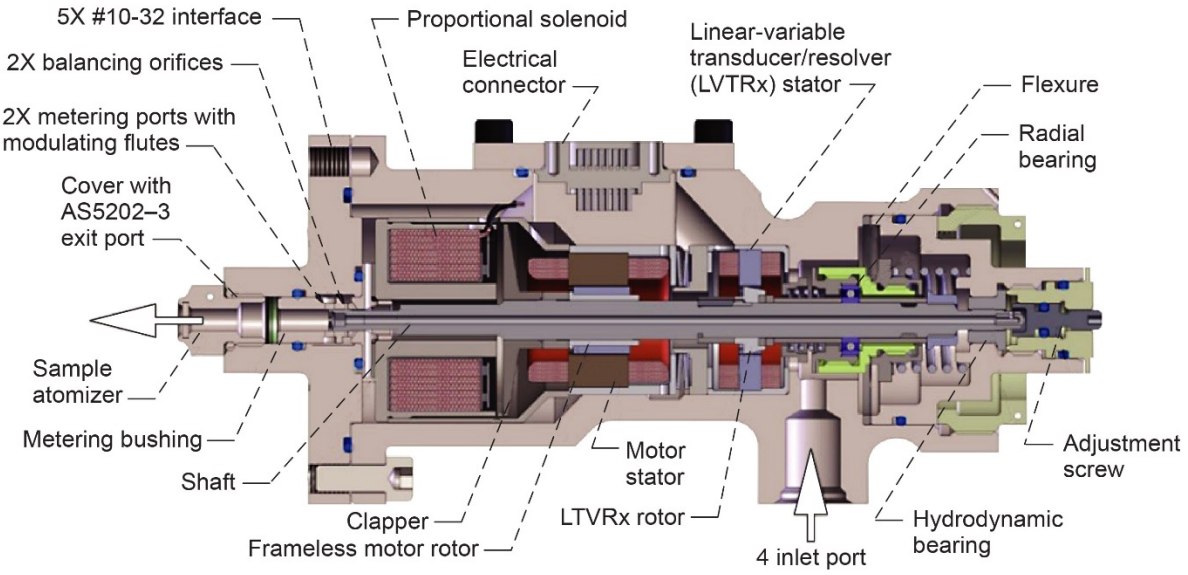

Figure 7.—Cutaway view of the JASC Modulator (from Ref. 23).

control box was supplied that provides for digital commands to the modulator and status for data acquisition. A square wave signal is used to command modulation frequency (shaft rotational speed), and a 0 to 10 V signal is used to control modulation amplitude (translation of the flutes relative to the stator windows). More detailed information about the description of the valve construction and operation is contained in the contractor's Final reports, cited in References 22 and 23. As was true for the ASM, these reports are not publicly available. To secure a copy of these references the reader must contact the contractor directly and make a formal request through them. The reference they provide may be redacted in some respects in order to protect information they consider proprietary. The contractor's address is provided as part of the reference as a convenience.

In the time since the modulator was delivered to NASA GRC in 2014, no performance data on the JASC modulator has been collected by NASA GRC. This is due in part to delays in obtaining an appropriate flow bench (fuel only) and then due to failures and malfunctions experienced during testing. The performance data presented below was reported by JASC and its partner United Technologies Research Center (UTRC). These tests were conducted at UTRC. Figure 8 shows a schematic of the test setup. Fuel was supplied to a positive displacement piston pump and its pressure and volumetric output was controlled by a bypass valve. The valve was manually operated to achieve a desired inlet pressure to the modulator by diverting flow back to the supply. A pressure transducer just upstream of the modulator inlet provided the necessary feedback. A flow meter and accumulator were also placed just upstream of the modulator inlet. The accumulator was used to attenuate pump noise and to provide general flow conditioning. The output of the modulator was directed into an atomizer. Extension tubes between the modulator exit and the atomizer were used during some tests to measure modulation degradation. In all cases the output of the atomizer was directed into plenum that was pressurized with nitrogen to simulate combustor back pressure. The discharged fluid was then directed back to the supply. Additional pressure transducers were placed at the modulator exit and just upstream of the atomizer inlet. The Active Combustion Control Valve (ACCV) controller shown is a bread board precursor of the Electronic Control Unit (ECU) that interfaces the Data Acquisition System (DAS).

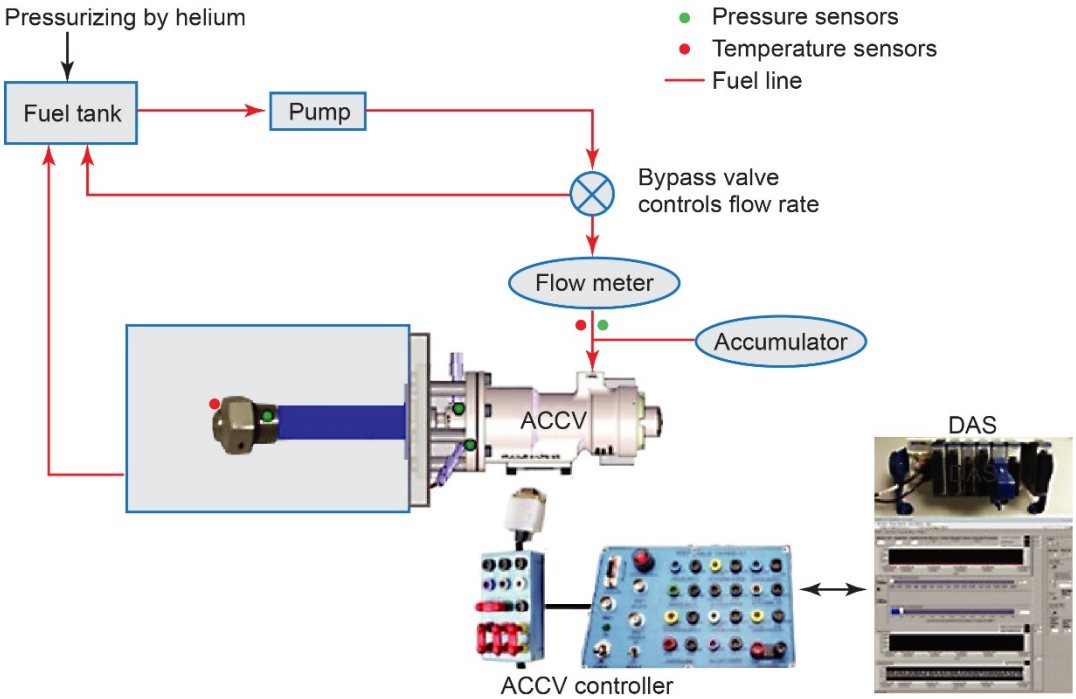

Figure 8.—JASC/UTRC Test Setup (from Ref. 23).

The data that was collected at UTRC was reduced in the form of frequency sweep plots of peak modulation strength percent versus frequency. The test conditions for which these plots were generated considered the effects of modulator inlet pressure, atomizer back pressure, and tube extension length for a fixed axial shaft position. The actual test matrix can be defined as all possible combinations for the following test variables:

Axial Shaft Position, x, $x \in \{0.01, 0.015, 0.02, 0.025\}\ inches$
Inlet Pressure, P_{in}, $P_{in} \in \{80, 160, 400, 800\}\ psi$
Back Pressure, P_{back} $P_{back} \in \{0, 200, 400\}\ psi$
Tube Length, L_{tube} $L_{tube} \in \{0, 6, 12, 18\}\ inches$

The modulator utilizes two rectangular flow ports, each having a total area of 9.639×10^{-4} in.^{2}. The flutes are also rectangular in shape. Their number and arrangement are such that the tops of the flutes cross each flow port in synchrony. It follows that the same is true for the flute root areas. For a given axial shaft position, there is a corresponding minimum and maximum area that the flow must pass through 16 times per revolution. These flow areas are summarized in Table 4 where Amin and Amax are percentages of the total flow port area.

Peak modulation strength percent, MS_{peak}, was calculated from atomizer flow. Equation (3), which is a reformulation of Equation (1), defines atomizer flow, W_f. This relationship describes the orifice equation where the mass flow, W_f (in lbm/hr), is proportional to the square root of the pressure difference across the orifice (in psid). The proportionality constant, FN, is the flow number. For the atomizer used in the testing, FN was empirically determined to be 2.94. Equation (4) shows the calculation of peak modulation strength percent over the frequency range tested. The ΔT subscript refers to the sweep time interval. For these tests the sweep interval was about 1 sec. $P_{\text{discharge}}$ refers to the exit pressure of the atomizer and P_{plenum} is synonymous with back pressure, P_{back}. The sweeps were logarithmic and spanned a frequency range of 200 to 1200 Hz.

$$W_f = \text{FN}\sqrt{\left(P_{\text{discharge}} - P_{\text{plenum}}\right)} \tag{3}$$

$$\text{MS}_{\text{peack}} = \frac{\text{mean}_{\Delta T}\left[\max\left(W_f\right)\right] - \text{mean}_{\Delta T}\left[\text{mean}\left(W_f\right)\right]}{\text{mean}_{\Delta T}\left[\text{mean}\left(W_f\right)\right]} \times 100 \tag{4}$$

Figure 9 and Figure 10 show the family of plots for the defined test matrix conditions for axial positions of 0.01 and 0.025 in., respectively.

TABLE 4.—MINIMUM AND MAXIMUM FLOW AREA AT A GIVEN AXIAL SHAFT POSITION

Axial position, in.	Amin, percent	Amax, percent
0.010	28.6	64.4
0.015	20.6	56.5
0.020	12.7	48.6
0.025	4.76	40.6

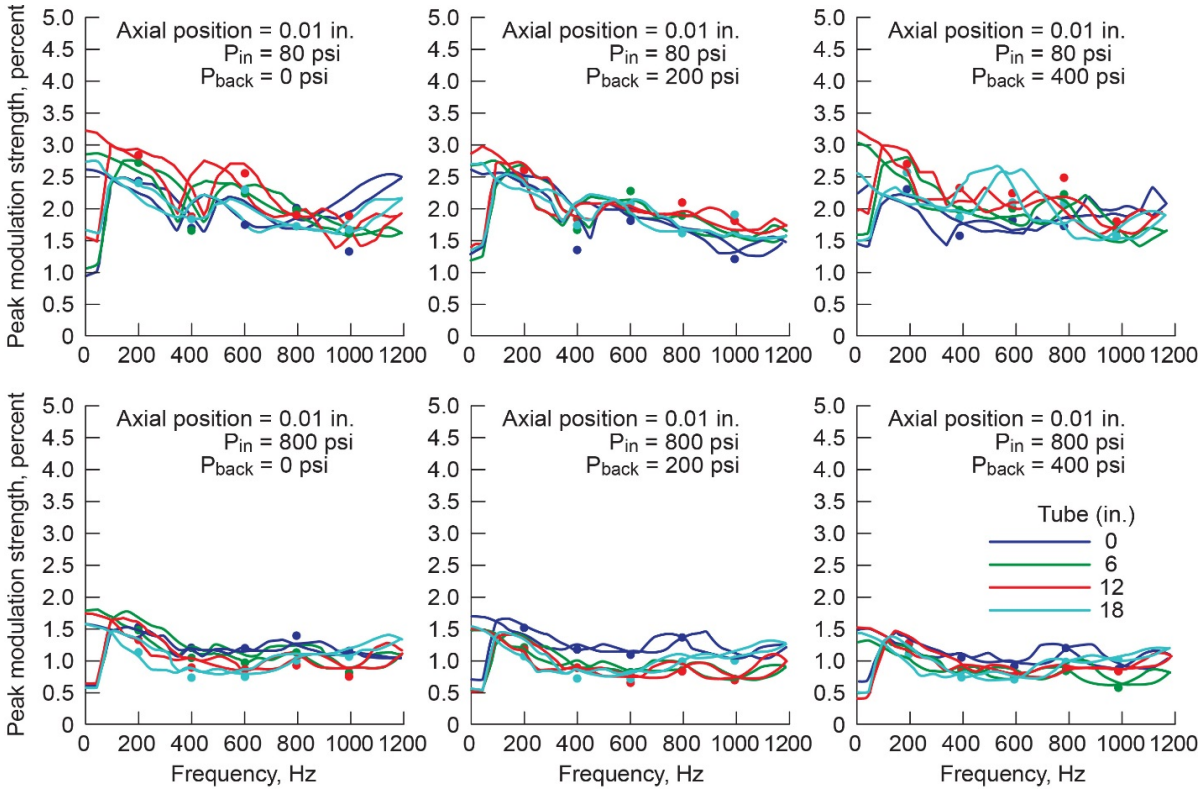

Figure 9.—Peak Modulation Strength for Various Inlet and Back Pressures and Tube Lengths at Axial Position 0.01 in. (from Ref. 23).

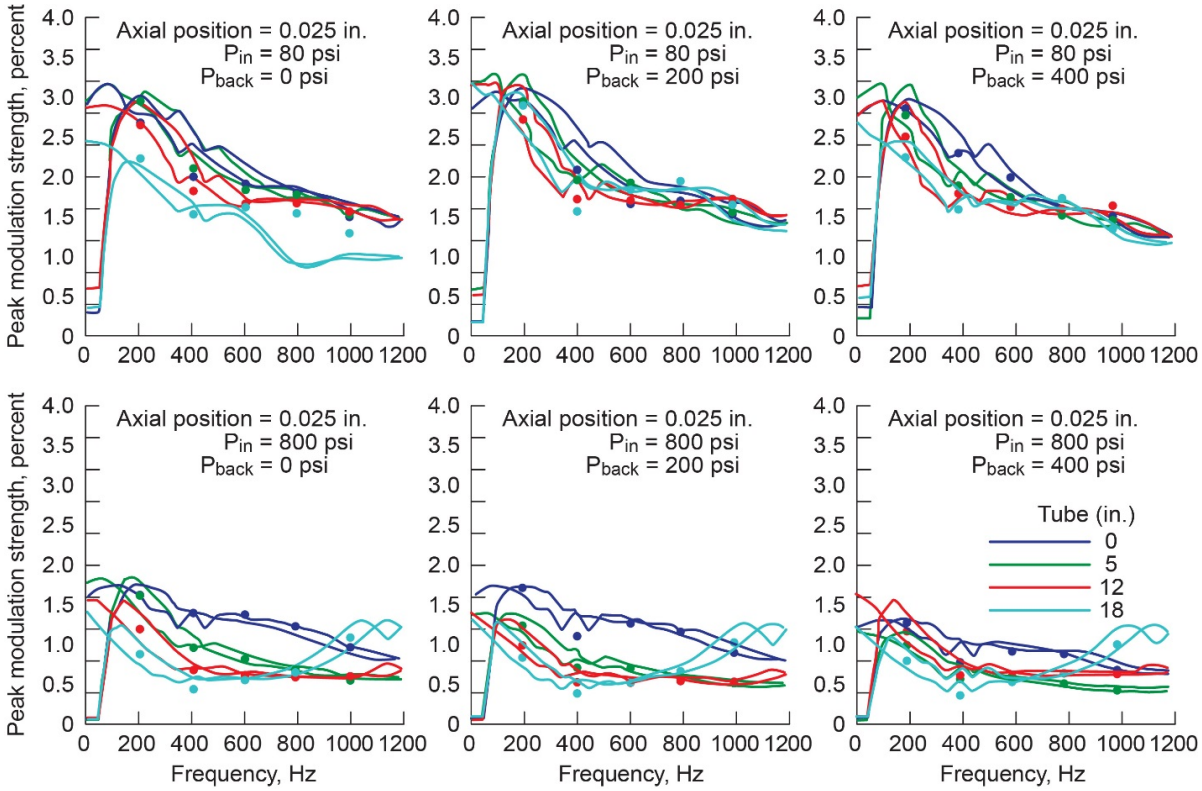

Figure 10.—Peak Modulation Strength for Various Inlet and Back Pressures and Tube lengths at Axial Location 0.025 in. (from Ref. 23).

The following observations can be made from the plots of peak modulation strength:

1. Inlet Pressure Effect—The modulation strength generally decreases as inlet pressure increases. This appeared consistently true for each family of plots. This effect is thought to be due to an increase in mean flow with an increase in inlet pressure while being mechanically limited to producing correspondingly higher ‘max’ flows relative to the new mean level.
2. Back Pressure Effect—No large variations are observed as back pressure increases.
3. Frequency Effect—For the 0.01 in. axial position families no large variations are observed; for the 0.025 in. axial position families, modulation strength tends to decrease as frequency increases.
4. Axial Position Effect—Modulation strength effectively increases with an increase in axial position.
5. Tube Length Effect—Modulation strength effectively decreases with an increase in tube length.

The WASK Engineering Modulator (WASK)

In the year 2012 another set of specifications for a high bandwidth fuel modulator were crafted by NASA GRC and incorporated into a SBIR solicitation. These specifications are listed in Table 5. The intent behind these specifications was to develop a modulator with a flow number capability that was on the order of a single fuel injector associated with a Lean Direct Injection array. Additionally, the goal was to develop a modulator that could be directly coupled with a fuel injector. This latter goal would eliminate modulation strength losses due to fuel pulse transmission along the line length from the remote installation location to the location of the fuel injector, but it would require a modulator design capable of surviving in a harsh temperature environment. Phase I and Phase II contracts were awarded to WASK Engineering for a proposed piezoelectric-based modulator design that incorporated a fuel cooling circuit. The modulator system that was developed is shown in Figure 11. The system components shown in the figure include a piezoelectric actuated modulator and a custom controller with its cover removed for clarity. Inferred from the photo of the controller, a 28 V power supply and a signal generator are required to make this modulation system operational.

Figure 12 shows an isolated view of the modulator (to be referred to as the WASK modulator in this section) that provides information on its volume. The first photo shows the modulator with an integrated concentric tube that provides a means by which fuel is supplied to the modulator and it also provides a conduit for the piezoelectric crystal power wires. The second photo isolates the modulator stack and shows its corresponding dimensions of about 2.8 by 0.6 by 0.6 in. Its weight is about 0.3 lb, most of which is accounted by the weight of the piezoelectric stack and the concentric stainless steel tube and fitting. Figure 13 shows a cutaway view of the modulator that identifies the fuel circuit, the feed wire conduit, the piezoelectric crystal, and the pintle/bellows (valving) leading to the fuel outlet.

TABLE 5.—DESIGN SPECIFICATIONS FOR WASK MODULATOR

Maximum mean flow rate	125 lbm/hr
Flow number range	1 to 5
Inlet pressure range	0 to 1000 psi
Minimum outlet pressure	250 psi
Desired modulation	±40% of mean mass flow
Minimum bandwidth	1000 Hz
Flow media	Water, JP-8 jet fuel
Maximum fuel inlet temperature	90 °F
Maximum operating temperature	1300 °F
Maximum volumetric dimensions	6 by 6 by 6 in.
Failure mode	Open

(a) WASK modulator.

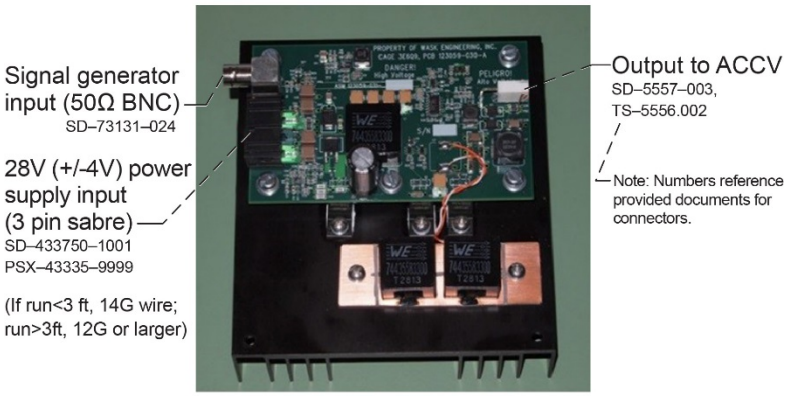

(a) WASK controller.

Figure 11.—The WASK Modulator and Controller (from Ref. 25).

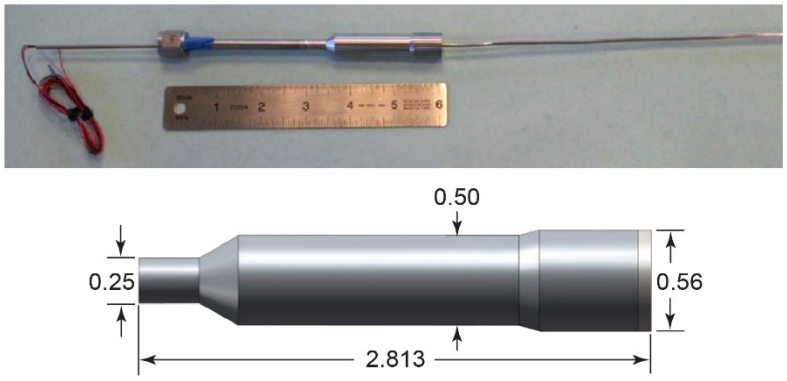

Figure 12.—Dimensional View of the WASK Modulator (from Ref. 25).

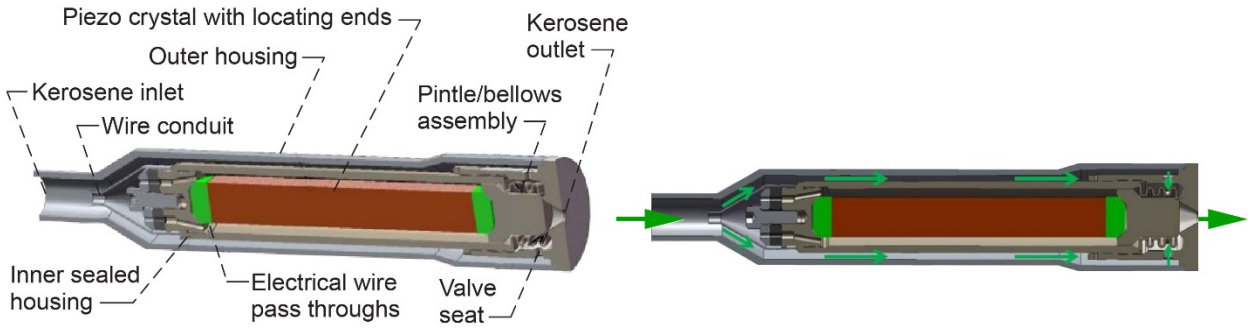

(a) WASK modulator cutaway. (b) Flow path of fuel through WASK modulator.

Figure 13.—Cutaway Views of WASK Modulator Showing Components and Flow Path (from Ref. 25).

In Figure 11 the controller is shown as requiring a source of electrical power and a signal source. The user uses the signal generator to provide a sinusoidal command signal to the controller which transmits the signal to the piezoelectric crystal. This voltage signal causes the crystal structure to strain which is observed as an axial displacement. Fuel enters the modulator housing and flows in a cavity that surrounds (but is isolated from) the crystal before entering another cavity constructed with bellowed walls. This flow serves as both a heat sink for the crystal as well as the supply for fuel modulation. Displacement of the crystal causes movement of an attached pintle that causes compression of the fluid in the bellowed cavity and the fluid is subsequently 'squirted' through the outlet. A concentric tube at the housing inlet serves as the fuel supply conduit (outer annulus) and as the conduit for piezoelectric crystal wires (inner annulus). More detailed engineering information for this modulator is contained in the vendor's final reports cited in References 24 and 25. Once again, these reports are not publicly available. To secure a copy of these references the reader must contact the contractor directly and make a formal request through them. The reference they provide may be redacted in some respects in order to protect information they consider proprietary. The contractor's address is provided as part of the reference as a convenience.

Characterization tests were conducted by WASK using the flow bench schematically shown in Figure 14 which is annotated with photos of actual hardware. The design parallels the NASA GRC short configuration design described in Figure 3 with the exception that the WASK design doesn't use a pressurized vessel to backpressure the downstream side of the simulated injection orifice. Rather,

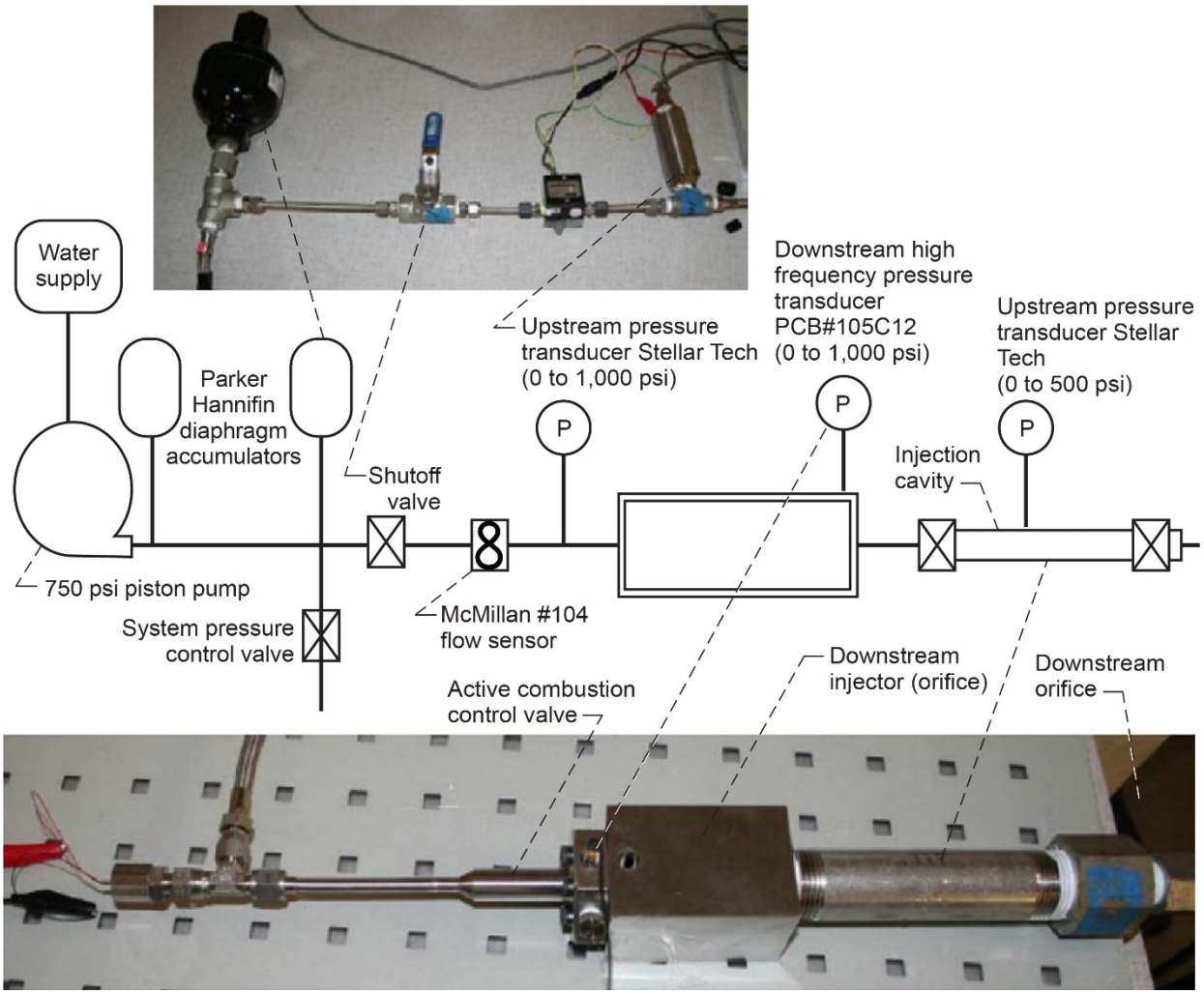

Figure 14.—Schematic of the WASK Flow Bench (from Ref. 25).

a ball valve is used downstream of the injection orifice for that purpose. The WASK system used a positive displacement piston pump and water was used as the working fluid. The output from a piston pump is quite noisy and so, for that reason, accumulators were used on its downstream side to attenuate oscillations in the fluid prior to reaching the inlet of the modulator. A ball valve upstream of the modulator was used to regulate system pressure by directing some of the pumped fluid to a drain. The shutoff valve was installed to facilitate the removal of the modulator from the system.

The fluid system being measured is a transient system and considered quasi-steady state. Both high and low frequency response pressure transducers were placed immediately upstream of the modulator (PD001 and PS001, respectively) and at the modulator exit (PD002 and PS002). The low frequency transducers are intended to measure the DC pressure level (they measure pressure absolutely); the high frequency transducers measure the AC level (they do not provide an absolute pressure measurement, just the displacement from the mean pressure). The sensing surfaces of the pressure transducers were oriented perpendicular to the fluid flow direction and were therefore making static measurements. The orifice simulating fuel injection was placed within 2 in. of the modulator discharge port. The downstream high frequency pressure transducer was placed midway between the discharge port and the orifice inlet. The downstream low frequency transducer was installed about 8 in. downstream of the downstream high frequency transducer, yet upstream of the downstream orifice that is used to control backpressure.

Figure 15 shows a calibration curve for the modulator resulting from the first flow test. A constant pressure of 300 psi water was established as the input supply to the modulator and then the input DC offset voltage was progressively increased (0 to 8.36 V – fully open to fully closed) to achieve incremental changes in crystal voltage of 20 V (0 to 100 V). The resulting curve of flow number as a function of input voltage is not strictly linear, but it does exhibit a linear trend. In consideration of this observation, the curve serves as a guide for determining the required DC offset voltage produced as an output of the signal generator necessary for establishing a mean flow rate (flow number). It should be noted that the piezoelectric crystal is still limited to 100 V, so the sum of commanded sinusoid amplitude voltage together with the DC offset voltage cannot exceed 8.36 V (signal generator voltage). This constraint poses a research question pertaining to the practical usage of this modulator as to how low of a flow number can be achieved and still have sufficient modulation amplitude available. The question is best answered empirically from combustion test data.

Signal generator voltage	Piezo actuator voltage	Valve flow coefficient Cv	Flow number Fn
0.00	0	0.00736	3.68270
1.67	20	0.00620	3.09978
3.35	40	0.00338	1.69074
5.02	60	0.00147	0.73494
6.69	80	0.00080	0.40221
8.36	100	0.00011	0.05499

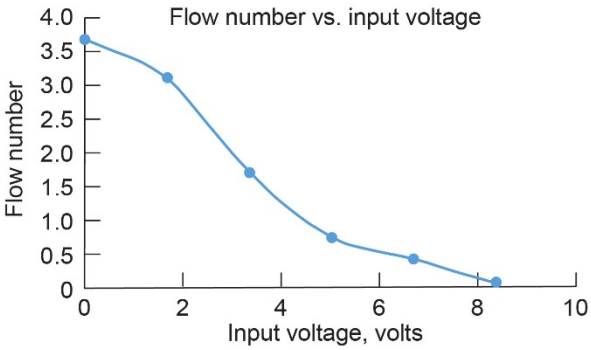

Figure 15.—Flow Number versus Input Voltage (from Ref. 25).

TABLE 6.—FLOW MODULATION TEST CONDITIONS

Inlet pressure, psig	Flow number	DC offset voltage, V	Amplitude, V	Frequency, Hz
344	0.386	4.18	4.10	250
346	0.403	4.18	4.10	500
345	1.25	4.18	4.10	750
345	1.057	4.18	4.10	1000

Table 6 lists the conditions for representative flow modulation tests conducted by WASK Engineering using sinusoidal command signals. The flow bench described in Figure 14 was used for these tests. An orifice having a flow number of 1 was used as the downstream injector orifice in the WASK setup. Figure 16 to Figure 19 show the results of the tests.

Figure 16 shows the result for modulation test at 250 Hz. In Figure 16(b), the upstream pressure measurement is shown having a relatively symmetric sinusoidal appearance (with frequency ~250 Hz) with a mean of approximately 343 psig and an amplitude of about 8 psig. The mean validates the inlet pressure condition; the sinusoidal appearance results from downstream modulated pressure waves being reflected upstream after encountering a hard boundary. For this modulation frequency, this 'low frequency' transducer has measured an amplitude that is comparable to the measurement of the 'high frequency' transducer shown in Figure 16(a). The most noticeable discrepancy between these two measurements is with regard to their phase, which appears to differ by as much as 180°. This is due to the spatial distance between the measuring locations for these two transducers. The mean of the downstream pressure shown in Figure 16(b) is around 341 psig which is about an average 2 psig drop across the modulator. Using this measurement and the FN listed in Table 6 for this condition in Equation (1), the mass flow rate is calculated as 0.55 lbm/hr. The general appearance of the downstream pressure (Figure 16(b)) is also a relatively symmetric sinusoid. Recall this measurement is taken downstream of the injection orifice. Its amplitude and general appearance differs somewhat from the measurement made upstream of the injection orifice (Figure 16(a)) which is about 8 in. away. The presence of harmonic frequencies is seen in both pressure traces, but they are more pronounced and of greater magnitude in the PD001 transducer. It should also be noted that the measurement from the PD001 transducer is not centered around zero. The vendor reported that discussions with the transducer supplier concluded that "A zero pressure measurement by the sensor does not necessarily indicate the average static pressure. Therefore, the overall downstream pressure variation, the difference between the maximum and minimum measured pressure values, is how the results should be interpreted." That said, the overall pressure variation indicated here is about 200 psig. That implies an amplitude swing of about ±100 psig. A 100 psig amplitude on top of a mean of 341 psig calculates as a modulation strength of 29.3 percent on a pressure basis. Recall, however, that this measurement is made immediately upstream of the injection orifice and so the amplitude of the pressure measurement made by PD002 (downstream of the orifice and 8 in. further down) may be a better indicator. For that measurement the amplitude is about 2 psig on top of a mean value of 341 psig. The modulation strength then calculates as 0.6 percent which indicates a significant attenuation! Figure 16(c) shows the power spectrum for the PD001 transducer measurement. The commanded frequency is the dominant frequency reported, but a number of harmonics are also present. This is very troublesome from an ACC perspective as the other harmonics can induce the creation of instabilities in the combustor other than the one being controlled. Note that employing a high frequency pressure transducer downstream of the orifice would have been helpful as a power spectrum of that measurement could be compared to determine whether the harmonics are eliminated as the modulation signal is attenuated. The scrutiny applied to this 250 Hz case can also certainly be applied individually to the plots for the remaining three frequencies. However, in lieu of this approach generalizations will be made in an attempt to characterize the modulator performance.

In Figure 17(b), Figure 18(b), and Figure 19(b), the upstream pressure measurement, PS001, consistently verifies the inlet pressure condition and it indicates the presence of a sinusoidal frequency. This is corroborated by its high frequency measurement counterpart, PD001, shown in plot ‘a’ for each of these respective figures. The magnitude of this sinusoidal amplitude, in comparison to that of the downstream pressure measurement, PD001, is considerably smaller, yet in comparison to the attenuated downstream measurement, PD002, it is very comparable. The inference here is that the modulator transmits the majority of the energy in the fuel pulse downstream, but it is quickly dissipated by the resistances posed by the orifice and fuel line. Another observation with respect to the upstream and downstream low frequency measurements is the magnitude of their mean. For the 250 and 500 Hz cases the mean of the upstream measurement was slightly greater than the mean of the downstream measurement. For the 750 and 100 Hz cases the reverse is true. This is presumed as being due to poor calibration of the sensor.

The amplitude of the sinusoidal measurement, PD001, is consistently in the 100 to 150 psig range for the frequencies shown and consistently dwindles to an amplitude of 1 psig or less in an 8 in. distance. The power spectrum plots for the PD001 measurement show the dominant frequency to be the commanded frequency, but with higher harmonics. This modulator was intended to be closely coupled with fuel injectors and the performance data would seem to indicate that it should be so since its modulation strength dissipates in a very short distance.

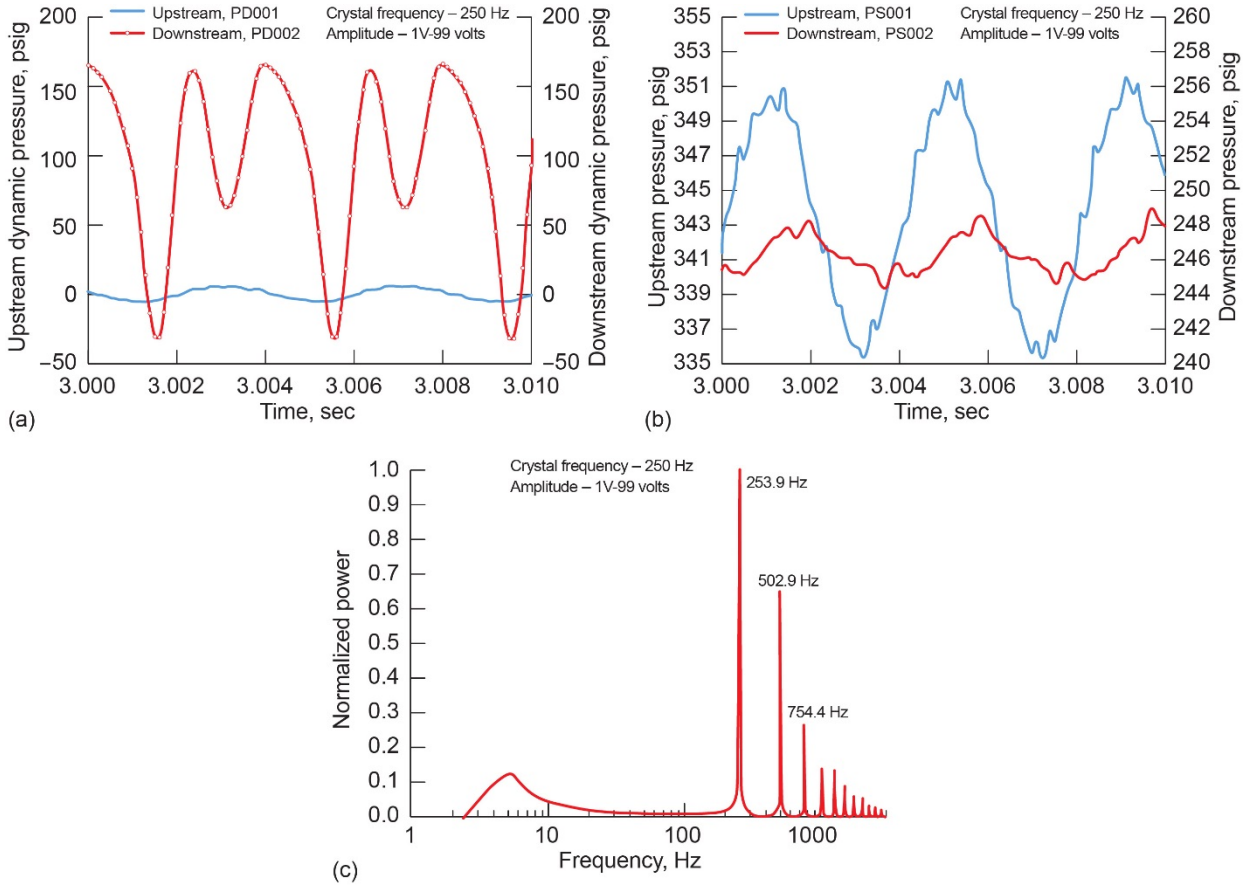

Figure 16.—Flow Modulation Test at 250 Hz (from Ref. 25).

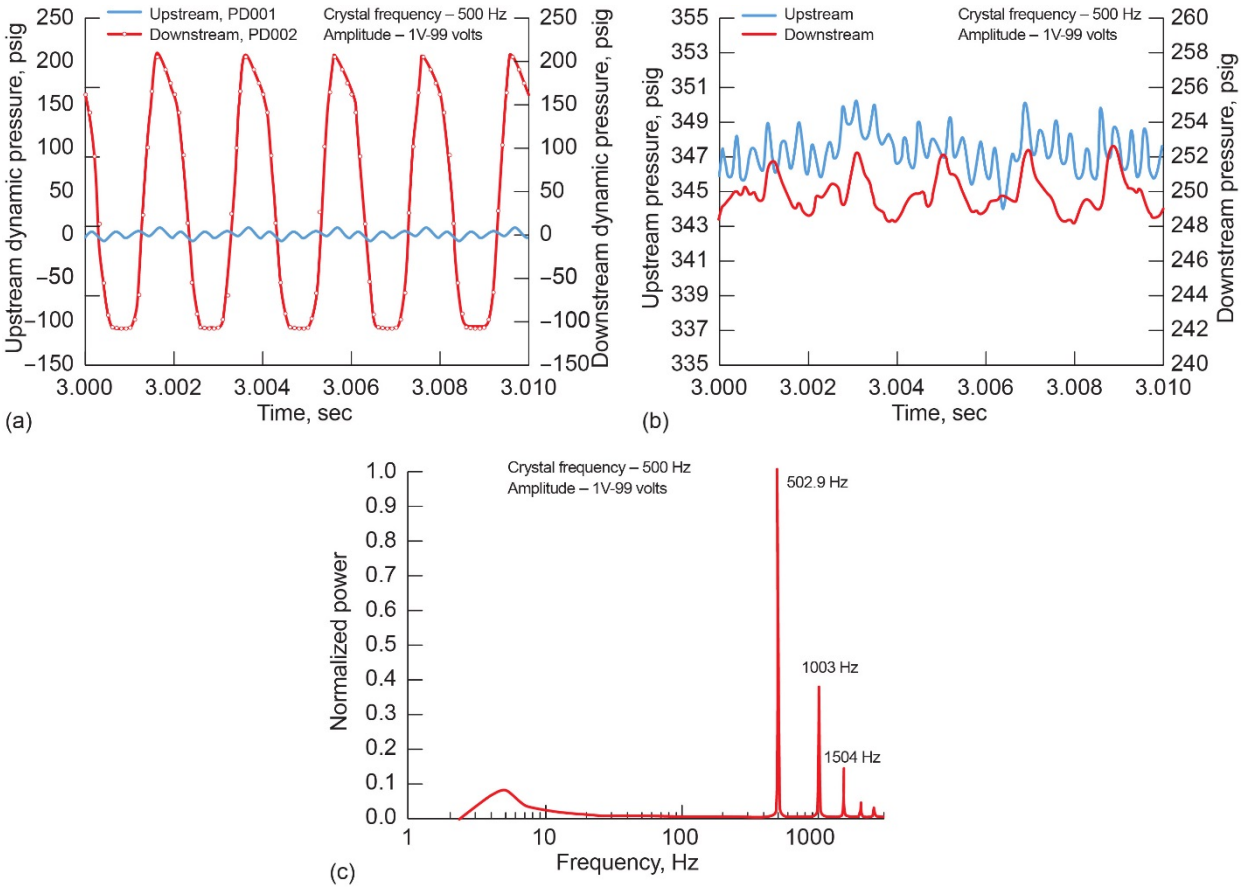

Figure 17.—Flow Modulation Test at 500 Hz (from Ref. 25).

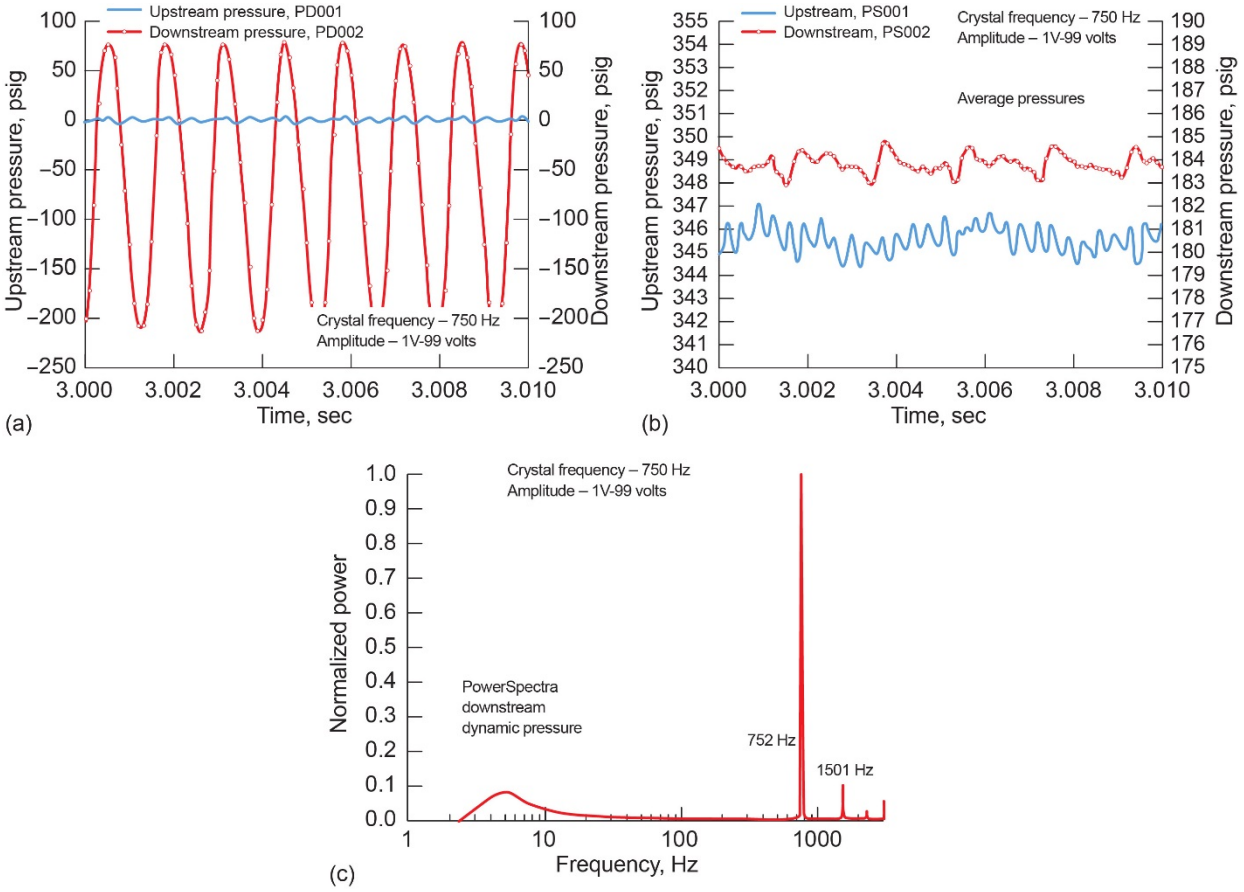

Figure 18.—Flow Modulation Test at 750 Hz (from Ref. 25).

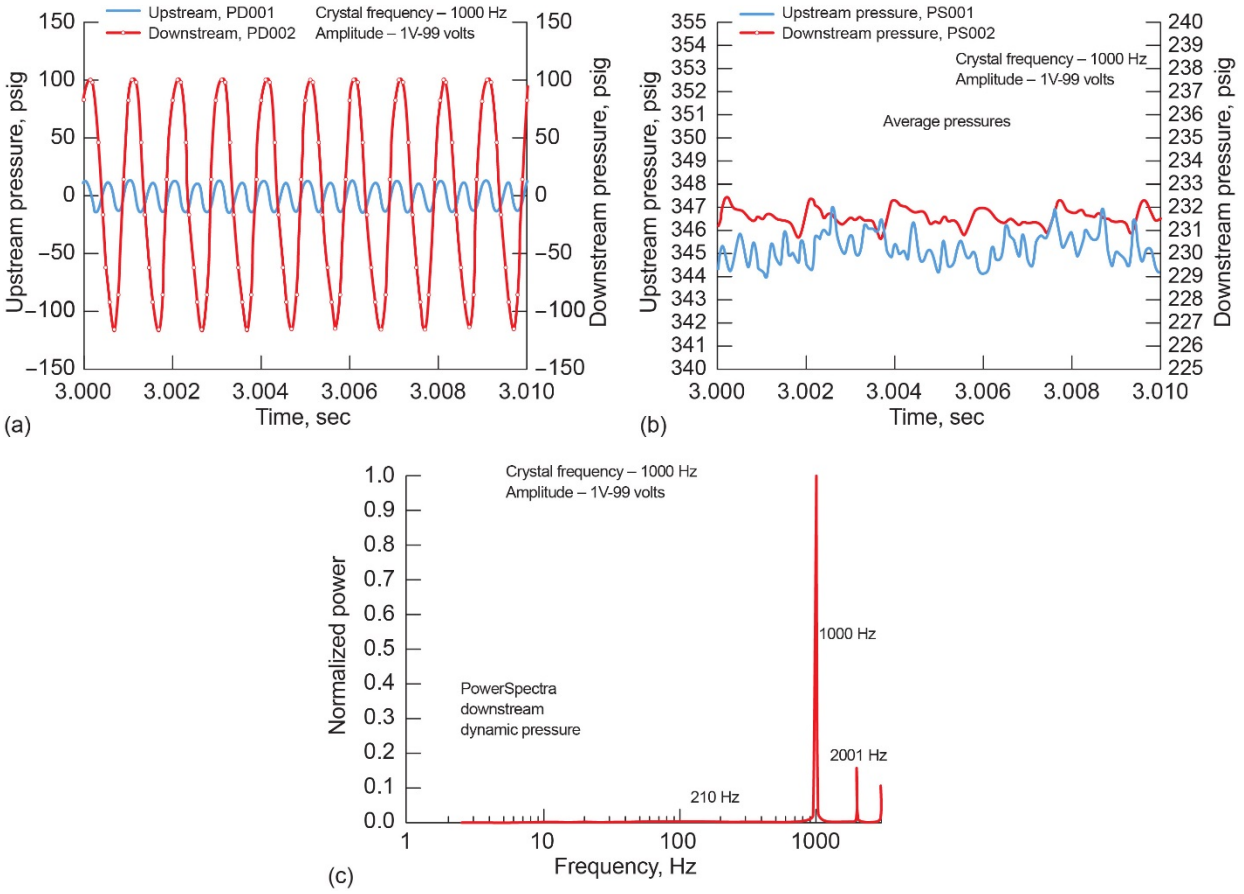

Figure 19.—Flow Modulation Test at 1000 Hz (from Ref. 25).

Conclusions and Future Work

The Georgia Tech Valve (GTV) demonstrated itself as an effective tool for Active Combustion Control (ACC) when main fuel supply modulation was implemented, but it was not effective for pilot supply modulation. This is because its nominal flow number design point prevented it from effectively operating at the lower flow numbers required for pilot flow modulation. For this reason the Active Signal Modulator (ASM), the Jansen's Aircraft System Controls (JASC) modulator, and the WASK Engineering modulator were procured. The focus of this paper has been to provide a cursory description of these latter modulators' physical construction and to describe their performance characteristics leading into actual ACC testing. The ASM and the JASC modulators have yet to be tested with actual combustion hardware due to hardware failures and/or malfunctions; the WASK modulator has been used in some tests, but the data is not complete for this publication. Laboratory performance tests that have been conducted on these devices indicate good potential for achieving a successful ACC implementation. The ASM modulator was tested under only a short configuration condition, so the amount of attenuation that can be expected with its generated fuel pulse prior to reaching the fuel injector remains an unknown. The WASK modulator was tested with long configuration conditions (8 in.), and exhibited significant attenuation of its fuel pulse. The JASC modulator was tested under long configuration conditions and the test results indicate suitability as a candidate for ACC research. As fuel modulation opportunities arise in combustion research facilities at the National Aeronautics and Space Administration Glenn Research Center (NASA GRC), these three devices will be individually selected based on the best fit for the research application.

References

1. Paxson, D.: "A Sectored-One-Dimensional Model for Simulating Combustion Instabilities in Premix Combustors," 38th Aerospace Sciences Meeting & Exhibit. AIAA-2000-0313, NASA TM-1999-209771, January 2000.
2. Cohen, J.M. et al: "Experimental Replication of an Aeroengine Combustion Instability," International Gas Turbine & Aeroengine Congress & Exhibition, Munich, Germany, ASME Paper 2000-GT-0093, May 2000.
3. Cannon, S.; Smith, C.; and Lovett, J.: "LES Modeling of Combustion Dynamics in a Liquid-Fueled Flametube Combustor," 36th Joint Propulsion Conference and Exhibit. AIAA-2000-3126, July 2000.
4. Nguyen, Q,: "Measurements of Equivalence Ratio Fluctuations in a Lean Premixed Prevaporized (LPP) Combustor and its Correlation to Combustion Instability," ASME Turbo Expo, Amsterdam, The Netherlands, ASME paper GT-2002-30060, June 2002.
5. Lieuwen, Tim, and Yang, Vigor, Combustion Instabilities in Gas Turbine Engines: Operational Experience, Fundamental Mechanisms, and Modeling, Published by AIAA, © 2006, *Vol. 210, Progress in Astronautics and Aeronautics Series*, 210.
6. Zinn, B.T.; Neumeier, Y.: "An Overview of Active Control of Combustion Instabilities," AIAA Paper 97-0461, January 1997.
7. McManus, K.R.; Magill, J.C.; Miller, M.F.; Allen, M.G.: "Closed-Loop System for Stability Control in Gas Turbine Combustors," AIAA Paper 97-0463, January 1997.
8. Schadow, K.; Yang, V.; Culick, F.; Rosfjord, T.; Sturgess, G.; Zinn, B.: "Active Combustion Control for Propulsion Systems," AGARD Report 820, September 1997.
9. Murugappan, S.; Aharya, S.; Gutmark, E.; Messina, T.: "Characteristics and Control of Combustion Instabilities in a Swirl-Stabilized Spray Combustor," 35th Joint Propulsion Conference and Exhibit, Los Angeles, CA. AIAA-99-31259, June 1999.
10. Hibshman, J.R.; Cohen, J.M.; Banaszuk, A.; Anderson, T.J.; Alholm, H.A.: "Active Control of Combustion Instability in a Liquid-Fueled Sector Combustor," International Gas Turbine & Aeroengine Congress and Exhibition, ASME Paper 99-GT-215, June 1999.
11. DeLaat, J.C.; Breisacher, K.J.; Saus, J.R.; Paxson, D.E.: "Active Combustion Control for Aircraft Gas Turbine Engines," 36th Joint Propulsion Conference and Exhibition, Huntsville, AL, AIAA-200-3500, NASA/TM—2000-210346, July 2000.
12. Kiel, B.: "Review of Advances in Combustion Control, Actuation, Sensing, Modeling and Related Technologies for Air Breathing Gas Turbines," 39th Aerospace Sciences Meeting and Exhibit, Reno NV, AIAA-2001-0481, January 2001.
13. Johnson, C.; Neumeier, Y.; Neumaier, M.; Zinn, B.; Darling, D.; Sattinger, S.: "Demonstration of Active Control of Combustion Instabilities on a Full-Scale Gas Turbine Combustor," ASME Turbo Expo 2001, New Orleans, LA. ASME Paper 2001-GT-0519, June 2001.
14. Annaswamy, A.M.; Ghoneim, A.F.: "Active Control of Combustion Instability: Theory and Practice," in *IEEE Control Systems Magazine*, Vol. 22, Num. 6, pp. 37–54, December 2002.
15. Kopasakis, G.; DeLaat, J.: "Adaptive Instability Suppression Controls in a Liquid-Fueled Combustor," 38th Joint Propulsion Conference and Exhibit, Indianapolis, IN, AIAA-2002-4075, NASA/TM—2002-21805, July 2002.
16. Kopasakis, G.: "High-Frequency Instability Suppression Controls in a Liquid-Fueled Combustor," 39th Joint Propulsion Conference and Exhibit, Huntsville, AL, AIAA-2003-1458, July 2003.
17. Le, D.; DeLaat, J.; Chang, C.: "Control of Thermo-Acoustic Instabilities: The Multi-Scale Extended Kalman Approach," 39th Joint Propulsion Conference and Exhibit, Huntsville, AL, AIAA-2003-4934, July 2003.
18. DeLaat, J; Kopasakis, G.; Saus, J.; Chang, C.; Wey, C.: "Active Combustion Control for Aircraft Gas-Turbine Engines – Experimental Results for an Advanced, Low-Emissions Combustor Prototype," 50th AIAA Aerospace Sciences Meeting including the New Horizons Forum and Aerospace Exposition, Nashville, TN, AIAA-2012-783, January 2012.

19. Saus, J.; DeLaat, J.; Chang, C; Vrnak, D.: “Performance Evaluation of a High Bandwidth Liquid Fuel Modulation Valve for Active Combustion Control,” 50th AIAA Aerospace Sciences Meeting including the New Horizons Forum and Aerospace Exposition, Nashville, TN, AIAA-2012-1274, January 2012.
20. Sewell, J.; Cooke, A.; Bridger, K.: “High Temperature, High Frequency Fuel Metering Valve,” NASA GRC SBIR Phase I Final Report, Contract #NNXCC64P, July 2009, Active Signal Technologies, 611 North Hammonds Ferry Rd., Linthincum, MD, 21090.
21. Bridger, K.; Cooke, A.; Kohlhafer, E.; Passaro, E.; Rubin, G.: “High-Temperature, High-Frequency Fuel Flow Modulation Valve,” NASA GRC NRA, Contract #NNC11CA10C, July 2012, Active Signal Technologies, 611 North Hammonds Ferry Rd., Linthincum, MD, 21090.
22. Caspermeyer, M.: “Novel Active Combustion Control Concept for High-Frequency Modulation of Atomized Fuel Flow,” NASA GRC SBIR Phase I Final Report, Contract #NNX10CC76P, July 2010, Jansen’s Aircraft Systems Controls, 2303 West Alameda Dr., Tempe, AZ, 85282.
23. Caspermeyer, M.: “Novel Active Combustion Control Concept for High-Frequency Modulation of Atomized Fuel Flow,” NASA GRC SBIR Phase II Final Report, Contract #NNX11CA44C, November 2013, Jansen’s Aircraft Systems Controls, 2303 West Alameda Dr., Tempe, AZ, 85282.
24. Burkhardt, W.: “Active Combustion Control Valve,” NASA GRC SBIR Phase I Final Report, Contract #NNX13CC22P, November 2013, WASK Engineering, 3905 Dividend Dr., Cameron Park, CA, 95682.
25. Burkhardt, W.: “Active Combustion Control Valve,” NASA GRC SBIR Phase II Final Report, Contract #NNX14CC22C, June 2016, WASK Engineering, 3905 Dividend Dr., Cameron Park, CA, 95682.